Journal of Back and Musculoskeletal Rehabilitation -1 (2021) 1–14 1
DOI 10.3233/BMR-200259
IOS Press

Brief Report

Musculoskeletal ultrasound for 3D bone modeling: A preliminary study applied to lumbar vertebra

A. Forbes[a,c], V. Cantin[c,d], Y. Develle[a], Y. Dubé[e], A. Bertrand-Grenier[f,g], C. Ménard-Lebel[a,c] and S. Sobczak[a,b,c,*]

[a]*Chaire de Recherche en Anatomie Fonctionnelle, Université du Québec à Trois-Rivières, Trois-Rivières (QC) Canada, G8Z 4M3, Canada*

[b]*Département D'anatomie, Université du Québec à Trois-Rivières, Trois-Rivières (QC) Canada, G8Z 4M3, Canada*

[c]*Groupe de Recherche sur les Affections Neuromusculosquelettiques (GRAN), Université du Québec à Trois-Rivières, Trois-Rivières (QC) Canada, G8Z 4M3, Canada*

[d]*Département des Sciences de L'activité Physique, Université du Québec à Trois-Rivières, Trois-Rivières (QC) Canada, G8Z 4M3, Canada*

[e]*Département de Génie Mécanique, Université du Québec à Trois-Rivières, Trois-Rivières (QC) Canada, G8Z 4M3, Canada*

[f]*Département de Chimie, Biochimie et Physique, Université du Québec à Trois-Rivières, Trois-Rivières (QC) Canada, G8Z 4M3, Canada*

[g]*CIUSSS de la Mauricie-et-du-Centre-du-Québec, Centre Hospitalier Affilié Universitaire Régional, Trois-Rivières, QC G8Z 3R9, Canada*

Received 8 September 2020
Accepted 10 February 2021

Abstract.
BACKGROUND: There is no non-invasive *in vivo* method to assess intervertebral kinematics. Current kinematics models are based on *in vitro* bone reconstructions from computed tomography (CT)-scan imaging, fluoroscopy and MRIs, which are either expensive or deleterious for human tissues. Musculoskeletal ultrasound is an accessible, easy to use and cost-effective device that allows high-resolution, real-time imaging of bone structure.
OBJECTIVE: The aim of this preliminary study was to compare the concordance of 3D bone modeling of lumbar vertebrae between CT-scan and ultrasound imaging and to study the intra and inter-reliability of distances measured on 3D ultrasound bone models.
METHODS: CT-scan, ultrasound, and *in situ* data of five lumbar vertebrae from the same human specimen were used. All vertebrae were scanned by tomography and a new musculoskeletal ultrasound procedure. Then, 3D bone modeling was created from both CT-scan and ultrasound image data set. Distances between anatomical bones landmarks were measured on the 3D models and compared to *in situ* measurements.

*Corresponding author: Professor S. Sobczak, Département D'anatomie de L'Université du Québec à Trois-Rivières, 3351, boul. des Forges C.P. 500, Trois-Rivières (Québec) Canada, G8Z 4M3, Canada. E-mail: stephane.sobczak@uqtr.ca.

RESULTS: We observed that all distances were included within the limit of agreement between the three methods of measurements (*3D CT-scan, 3D MSU and in situ*) with a good intra- and inter-reliability of 3D ultrasound measurements of 0.97 and 0.82, respectively. Based on the mean of mean differences between methods, we observed for all distances, ultrasound overestimated distances of 0.44 ± 0.63 mm compared to CT-scan, ultrasound underestimated distances of 0.39 ± 0.48 mm compared to *in situ* measurements and CT-scan underestimated distances of 0.93 ± 0.55 mm compared to *in situ* measurements.
CONCLUSIONS: Three-dimensional modeling from ultrasound imaging is similar in comparison to 3D bone modeling from CT-scan imaging with a good intra and inter reliability.

Keywords: Musculoskeletal ultrasound, computed tomography, three-dimensional reconstruction, lumbar vertebrae, bone modeling

1. Introduction

Of all musculoskeletal health problems, back pain is one of the most prevalent as nearly 85% of the population will experience non-specific low back pain (LBP) in their life with important human and material costs related [1,2]. It has been reported that a loss of intervertebral height will decrease the intervertebral mobility which is the first causes of LBP, but some of the underlying mechanisms remain unclear [3]. To improve LBP assessment and to evaluate effects of LBP rehabilitation, clinicians need new tools to determine spine kinematics.

Today, there is no non-invasive method to determine *in vivo* intervertebral spine kinematics. Lumbar spine displacement is assessed by physical examination, which is subjective, by optical tracking systems and imaging studies that typically include multiple-planar fluoroscopy, computed tomography (CT)-scan imaging, or magnetic resonance imaging (MRI). All these methods are limited by radiation exposure, equipment size, power requirements, and/or inaccuracies introduced by skin motion artifacts [4]. Current kinematics models are based on bone reconstructions from CT-scan imaging, fluoroscopy and MRIs, which are either deleterious for human tissues or expensive [5–13]. Concerning joint kinematics, CT-scan bone modeling is still considered as gold standard but the use of this method, *in-vivo*, is not appropriate [14,15]. A previous study reported that low dose computed tomography did not affect the quality of reconstructions and the amount of radiation did not alter patient-specific 3D bone modeling [16]. Even if the amount of radiation did not alter 3D bone modeling, the localization of bone landmarks on this 3D models has a significant impact on joint kinematics. Improving the reliability of this localization will improve the joint axes determination [17].

Although new medical imaging tools such as 3D ultrasound are appearing last decade. They are still expensive and not easily accessible for use in most clinics and research centers [18–20]. Getting 3D bone modeling is important to describe an anatomical coordinate system which is essential to determine both, vertebral rotations and translations. Presently, all 3D ultrasound systems are not implemented to determine spine kinematics. To improve research and offer a greater possibility of diagnostic tools, it becomes interesting to combine a common and less expensive clinical tool as 2D musculoskeletal ultrasound (MSUS) and develop easy fusion algorithm to get a 3D environment and then define 3D intervertebral kinematic thanks to 3D bone modelling based on MSUS imaging.

MSUS is an accessible, easy to use and cost-effective diagnosis device that allows high-resolution, real-time imaging of bone structure [21–24]. It has not been used to its full potential and the search for new applications is still a topic of interest for many researchers [23,25]. MSUS has been previously used to determine vertebral motion but only by describing 2D landmarks displacement. There are relatively few articles reporting the use of ultrasound for motion determination. Chleboun et al. assessed the lumbar extension amplitudes with 2D ultrasound by measuring distance variations between the spinous processes [26]. Others have measured the amplitudes of movement along the three anatomical planes by introducing external fixator equipped with a triple extracorporeal ultrasound sensor into the spinous processes of healthy subjects' vertebrae [27]. Wand et al. reported high intra and inter-rater reliabilities and agreements between 3D ultrasound and MRI in determining positions of vertebral rotation in the transverse plane for scoliosis patients [18]. Sobczak et al. studied ultrasound validity to measure the *in vitro* lumbar spine vertical displacement in comparison with caliper measurements [28]. They obtained intraclass correlation coefficients ranged from 0.98 to 1 (intra and interobserver) and confidence intervals within the limits of agreement between the two measurement methods. Recently, a new method has been reported that enables accurate tracking of the relative motion of contiguous cervical

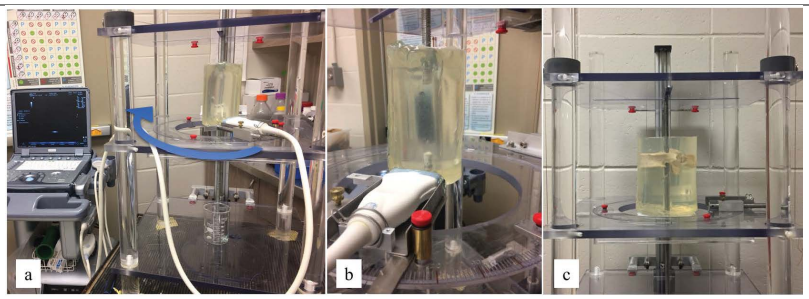

Fig. 1. (a) Computer-assisted mechanical frame (CAM) with the probe position on the mobile plate; (b) phantom model and (c) vertebra located in the CAM center after gelatin hardening.

vertebrae from ultrasound radio-frequency data [29]. They reported the surrounding tissue did not affect the ultrasound radio-frequency data using B mode. However, all these studies related to the use of ultrasound technology allow to determine 2D displacement and do not allow to determine 3D joint kinematics.

According to the literature there is a need to develop in a near future a kinematic tool to determine 3D lumbar kinematics thanks to MSUS imaging. As reported, spinal kinematic have to be based on 3D bone modeling on which an anatomical coordinate system must be created. In this case the first step is to assess if MSUS allow to create 3D bone modeling. We hypothesize that 3D modeling from MSUS images would be similar to those obtained by CT-scan. The aims of this study were (1) to compare the concordance between bones distances measured on 3D modeling of phantom models and lumbar vertebrae between CT-scan, MSUS imaging and *in situ* caliper measurement and (2) to study the intra and inter-reliability of these distances measured on 3D bone modeling from MSUS imaging.

2. Methods

2.1. Computer-assisted mechanical frame

A computer-assisted mechanical frame (CAM) (Fig. 1a) was custom-built for this study. The CAM ensured the MSUS probe displacement standardization (velocity) during MSUS data collection (Fig. 1). A mobile plate and a stepper motor were attached to the CAM frame. The stepper motor was controlled by a laptop using a configuration software (SureStep Pro^{TM} AutomationDirect, Atlanta, GA, USA). The vertical displacement was set as needed depending on the dimension of the object (phantom models or vertebrae) to scan. The center of the mobile plate had a circular hole with a diameter of 20 cm and allowed to place both, phantom models and vertebrae in its center. The MSUS probe was fixed on the mobile plate. The mobile plate was able to turn around the vertical axis with increments of 1 degree. To stabilize firmly objects to scan, metal threaded rods were used. Concerning vertebrae, vertebral foramina were filled out with epoxy resin. Threaded rods were screwed in their center.

2.2. Gelatin molding

Prior to each acquisition of ultrasound data, phantom models and vertebrae were stabilized on the threaded rods, then individually immersed in porcine gelatin (Gelatin, Type A, Pork Skin, min. Bloom 225). After gelatin hardening, objects to scan were placed in the center of CAM. The gelatin ensures ultrasounds conduction (Fig. 1b and c).

2.3. Validation on phantom models

Two Plexiglas cylinders (50 $\times$ 100 mm and 38 $\times$ 100 mm) were used as phantom models to develop and validate the US modeling method. Cylinders were manufactured at hundredth millimeters at our mechanical department. CT-scan images from both cylinders served as 'gold standard' [16] to allow comparison with ultrasound images.

2.4. Data acquisition

Dry vertebrae from L1 to L5 from the same specimen (male aged 64 years) from our personal collection were used. Prior to data collection the study was approved by the local ethics subcommittee (SCELERA-18-045). CT-scan images were collected thanks to a Somatom4 (Siemens, helical mode, reconstruction: slice thickness = 0.5 mm, inter-slice spacing = 0.5 mm, image data format = DICOM) at the hospital center of Trois-Rivières. Ultrasound images (NextGen LOGIQ

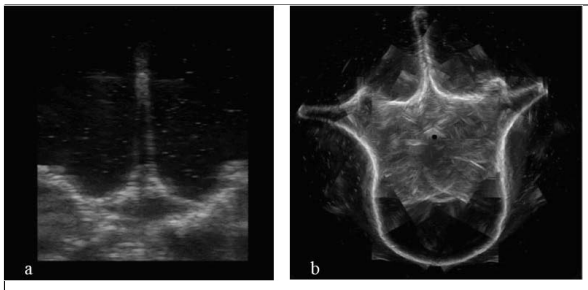

Fig. 2. Ultrasound images before (a) and after images fusion (b).

e Ultrasound, GE Healthcare, USA – Mode = Musculoskeletal, Frequency = 8.0 MHz, Distance = 6 cm, Gain = 76) were collected in our anatomy laboratory. Cylinders data imaging were obtained with a 12 cm linear vertical displacement of the probe (displacement velocity: 0,48 mm/s), resulting in a 383 images files. Transversal displacement (rotation around the central axis) consisted of 9 sets of images, which were taken at every 40-degrees position (0 to 320 degrees). As the vertebrae were more complexes than cylinders, transversal displacement was adjusted to 12 sets of images, which were taken at every 30-degrees from 0 to 330 degrees to ensure 3D bone modeling. Vertical displacement was reduced to 8 cm to limit the size of the files (181 images/data set).

2.5. *Segmentation and three-dimensional modeling*

Prior to 3D modeling, images for each vertical position were fused using a homemade script in Matlab (Mathworks, R2017a). The result was a single file of new 360-degrees dicom images for each vertebrae and cylinders (Fig. 2). All new images were created thanks to the size of MSUS images (Depth and width in px) and both, the radius of mobile plate and the distance between the probe and the center of the mobile plate. 3D segmentation and 3D bones and cylinders modeling were performed using Amira software (Amira 5.2.2®, Germany). Voxel conversion for each model was determined by using the X and Y pixel values (in millimeters) from the resulting planar images. MSUS data are planar. Z (vertical) conversion was obtained using the velocity, height and number of images per second from the data acquisitions.

2.6. *Bones landmark localisation and distance measurements*

CT-scan and MSUS distance measurements were collected based on precise bone landmarks (Fig. 3): D1

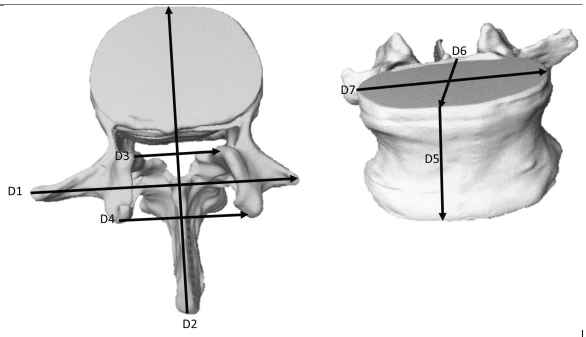

Fig. 3. Landmarks used for distance measurements. D1 = The most lateral point of the left costiform process (the ventral root of the lumbar transverse process) to the most lateral point of the right costiform process; D2 = Anterior vertebral body limit to the most posterior point of the spinous process; D3 = Medial limit of the superior articular processes (left to right, anterior limit); D4 = Superior articular process (left to right, posterior limit); D5 = Body thickness of the anterior side; D6 = Antero-posterior vertebral body length; D7 = Medio-lateral vertebral body length.

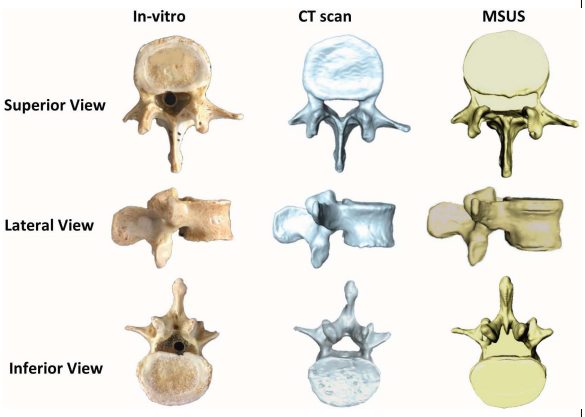

Fig. 4. *In vitro*, Ct-Scan and MSUS representation of the second lumbar vertebra.

= The most lateral point of the left costiform process (the ventral root of the lumbar transverse process) to the most lateral point of the right costiform process; D2 = Anterior vertebral body limit to the most posterior point of the spinous process; D3 = Medial limit of the superior articular processes (left to right, anterior limit); D4 = Superior articular process (left to right, posterior limit); D5 = Body thickness of the anterior side; D6 = Antero-posterior vertebral body length; D7 = Medio-lateral vertebral body length. Measurements were carried out on 3D models thanks to the measurement's tools of AMIRA. For better comparisons of CT-scan and US 3D bone modeling, we also took measurements directly on the vertebrae using a digital caliper (CAL) (Mitutoyo Absolute Digital Caliper, 0.01 mm accuracy, 0–100 mm measuring range, Japan). This allowed to in-

Table 1

Mean (X), Standard deviation (SD), coefficient of variation (%) and Mean differences (MD) with Standard Error (SE) and Confidence Interval [95% CI] values of distances (mm) collected on cylinders. Negative Mean difference values mean the distances measured by the compared method were higher

		38 mm			50 mm		
		CAL	CT Scan	MSUS	CAL	CT Scan	MSUS
Length	X	99.97	97.81	99.47	100.03	97.76	99.94
	SD	0.16	0.10	0.07	0.05	0.07	0.10
	CV	0.16	0.10	0.07	0.05	0.07	0.10
	CAL – Ct-Scan						
	MD	2.16			2.27		
	SE	0.13			0.04		
	CI	[1.91 2.41]			[2.20 2.35]		
	CAL – MSUS						
	MD	0.50			0.09		
	SE	0.09			0.05		
	CI	[0.32 0.67]			[−0.02 0.19]		
	Ct-Scan – MSUS						
	MD		−1.67			−2.18	
	SE		0.06			0.02	
	CI		[−1.79 −1.54]			[−2.23 −2.14]	
Width	X	37.99	36.16	36.19	50.00	48.90	51.16
	SD	0.13	0.17	0.08	0.05	0.07	0.20
	CV	0.34	0.47	0.22	0.10	0.14	0.39
MD	*CAL – Ct-Scan*						
	MD	1.83			1.10		
	SE	0.14			0.03		
	CI	[1.57 2.09]			[1.03 1.17]		
	CAL – MSUS						
	MD	1.80			−1.16		
	SE	0.05			0.11		
	CI	[1.69 1.9]			[1.37 −0.95]		
	Ct-Scan – MSUS						
	MD		−0.03			−2.26	
	SE		0.11			0.11	
	CI		[−0.25 0.19]			[−2.48 −2.04]	

tegrate a third measurement method, as control, for our statistical analysis (Fig. 4). Concerning cylinders, diameters and lengths were measured following the same procedure.

2.7. Measurements

Concerning the reliability, each measurement was repeated five times on both CT-scan and MSUS 3D bone modeling, as well as on the vertebrae with the digital caliper. To assess intra-rater reliability of distance measurements on MSUS 3D bone modeling, the same rater performed new 3D modeling of vertebrae before assessing the measurement protocol. This measurement protocol was repeated within- and between-days: three times on the same day and on a three-day interval. Concerning inter-raters reliability, three raters applied the same measurements only on one set of MSUS modelization. Concerning methods agreement, measurements on cylinders, 3D Bone modeling from CT-scan, MSUS and *in situ,* one rater measured all distances five times on the fives vertebrae with two days interval each.

2.8. Statistical analysis

Mean difference (MD), standard deviation (SD) and coefficient of variation (CV) were assessed for each distance. Standard errors (SE) and 95% coefficient intervals (CI) between CT-scan, MSUS and CAL measurements of both cylinders were calculated, then the same analysis were made on vertebrae data. Limits of agreement between methods considering all vertebrae as a whole sample were calculated using Bland and Altman method [30–32]. According to the results of SE, CI and Bland and Altman analysis, we decided to assess the intra- and inter-rater reliability by applying intraclass correlations coefficient (ICC – 2.1 Two-Way random) on distances measured only on 3D MSUS bone reconstruction with 95% CI. All statistical analyses were performed with SPSS software (SPSS Statistics for Windows, version 24.0; IBM Corp., Armonk, NY, USA).

3. Results

3.1. Validation on cylinders

In comparisons to caliper measurements (Table 1), mean differences for both, length and width of the 38 mm cylinder were respectively 0.50 and 1.80 mm for MSUS measurements, 2.16 and 1.83 mm for CT-scan measurements. Mean differences for both, length and width of the 50 mm cylinder were respectively 0.09 and −1.16 mm for MSUS measurements, 2.27 and 1.10 mm for CT-scan measurements. In comparisons to CT-scan measurements, mean differences for both, length and width of the 38 mm cylinder were respectively −1.67 and −0.03 mm and for the 50 mm cylinder, length and width were respectively −2.18 and −2.26 mm for MSUS measurements. Standard errors calculated on the mean difference were ranged from 0.04 to 0.14 mm. Mean values, standard deviations, coefficients of variation and 95% CI are also reported in Table 1.

3.2. Concordance of distance measurements from 3D modeling and in situ measurement

Table 2 reports all distances on lumbar vertebrae from L1 to L5 and for all methods. Concerning CT-scan, MSUS and CAL, coefficients of variation were ranged from 0.15% to 2.11%, from 0.18% to 3.25% and from 0.05 to 3.42%, respectively. Mean CV (SD) for CT-scan, MSUS and CAL were 0.67% (0.49%), 1.11% (0.93%) and 0.58% (0.69%), respectively.

For each comparison (CT-scan/MSUS, CAL/CT-scan, CAL/MSUS) and for all measurements, Table 3 reports all mean differences with 95% CI. We wanted to observe if variations were dependent of the anatomical plans in which distances were collected (transversal, antero-posterior and vertical). Concerning MSUS measurements for antero-posterior distances (D2, 6), Mean MD showed a slightly overestimation in comparison to CT-scan (MD: -0.81 ± 1.11 mm) and *in situ* (-0.05 ± 0.87 mm). Concerning transversal distances (D1, 3, 4, 7), Mean MD showed a slightly overestimation in comparison to CT-scan (MD: -0.78 ± 1.76 mm) and underestimate *in situ* measurements (0.13 ± 1.29 mm). Finally, about the vertical distance (D5), Mean MD showed a slightly overestimation in comparison to CT-scan (MD: -0.16 ± 0.99 mm) and underestimate *in situ* measurement (0.86 ± 0.91 mm). Based on the mean MD these distances modifications are all below 1 mm with a higher modification for MSUS in vertical axis.

Table 2
Mean (X), standard deviation (SD) and coefficient of variation (%) of distances (mm) collected on 3D bone modeling and *in situ*

		Distances						
		D1	D2	D3	D4	D5	D6	D7
					Ct-Scan			
$L1$	X	71.5	88.3	19.4	28.1	27.8	35.1	46.3
	SD	0.20	0.22	0.17	0.34	0.25	0.30	0.09
	CV	0.28	0.25	0.88	1.23	0.89	0.86	0.19
$L2$	X	80.2	93.2	25.2	29.3	28.7	38.0	49.5
	SD	0.31	0.15	0.45	0.29	0.48	0.28	0.13
	CV	0.38	0.16	1.77	1.00	1.68	0.74	0.26
$L3$	X	94.3	93.1	20.7	32.9	28.9	38.0	52.2
	SD	0.32	0.57	0.44	0.23	0.11	0.23	0.08
	CV	0.34	0.62	2.11	0.70	0.37	0.60	0.15
$L4$	X	67.4	88.8	24.6	35.2	29.8	37.0	55.6
	SD	0.14	0.17	0.34	0.10	0.35	0.33	0.19
	CV	0.21	0.20	1.40	0.27	1.16	0.88	0.34
$L5$	X	90.9	85.1	23.3	51.4	26.8	41.0	58.6
	SD	0.41	0.24	0.15	0.17	0.15	0.30	0.25
	CV	0.45	0.28	0.66	0.33	0.55	0.74	0.43
					MSUS			
$L1$	X	75.7	86.8	19.1	27.0	27.2	34.8	46.1
	SD	0.15	0.34	0.40	0.24	0.06	0.51	0.27
	CV	0.20	0.39	2.08	0.90	0.22	1.45	0.58
$L2$	X	79.6	93.4	24.8	29.5	29.8	37.3	49.4
	SD	0.67	0.67	0.47	0.96	0.24	0.33	0.09
	CV	0.84	0.72	1.91	3.25	0.79	0.88	0.18
$L3$	X	96.9	93.2	20.0	33.3	28.6	38.7	52.1
	SD	0.25	1.28	0.26	0.70	0.89	0.21	0.42
	CV	0.25	1.38	1.30	2.09	3.11	0.54	0.82
$L4$	X	69.8	90.4	24.4	35.8	31.0	38.6	57.9
	SD	1.06	0.45	0.47	0.10	0.09	0.87	0.67
	CV	1.52	0.49	1.94	0.28	0.28	2.26	1.16
$L5$	X	95.4	85.7	23.9	52.7	27.7	41.4	61.9
	SD	0.43	0.27	0.31	0.19	1.02	0.23	0.30
	CV	0.45	0.31	1.30	0.35	3.70	0.56	0.48
					CAL *(In situ)*			
$L1$	X	72.8	88.5	19.5	28.4	28.3	35.3	46.5
	SD	0.08	0.07	0.20	0.44	0.08	0.09	0.11
	CV	0.10	0.08	1.01	1.56	0.27	0.26	0.24
$L2$	X	79.5	94.0	25.5	29.3	29.5	37.8	51.7
	SD	0.26	0.48	0.25	0.04	0.04	0.12	0.12
	CV	0.32	0.51	0.98	0.13	0.15	0.32	0.24
$L3$	X	97.1	95.8	21.1	32.8	31.0	38.8	53.7
	SD	0.05	0.35	0.72	0.07	0.10	0.22	0.14
	CV	0.05	0.36	3.42	0.20	0.33	0.56	0.26
$L4$	X	69.6	90.0	24.7	35.5	30.5	37.5	57.8
	SD	0.07	0.21	0.38	0.37	0.20	0.32	0.10
	CV	0.10	0.24	1.54	1.05	0.65	0.85	0.18
$L5$	X	93.0	85.6	23.8	51.3	27.8	42.0	61.2
	SD	0.09	0.18	0.51	0.28	0.22	0.22	0.05
	CV	0.09	0.21	2.13	0.55	0.80	0.53	0.09

Considering all vertebrae as a whole sample, limits of agreement (Table 4) and Bland and Altman plots (Fig. 5) demonstrated comparisons were included in the limits of agreements excepted for D1 (costiform to costiform) at L5 especially for MSUS measurement where distance was overestimated (Table 3 – MD: −5.79 and −3.64). Means MD (SD) were -0.44 ± 0.63 mm, 0.83

Table 3
Mean differences (MD), Standard Error (SE) and Confidence Interval [95% CI] for all distances and vertebrae. Negative MD values mean the distances measured by the compared method were higher. All values are in mm

		Ct-Scan vs MSUS			CAL vs Ct-Scan			CAL vs MSUS		
		MD	SE	CI	MD	SE	CI	MD	SE	CI
D1	L1	−1.26	0.11	[−1.47 −1.05]	1.32	0.09	[1.15 1.49]	0.06	0.12	[−0.18 0.30]
	L2	1.17	0.23	[0.72 1.61]	−0.71	0.23	[−1.16 −0.25]	0.46	0.02	[0.41 0.51]
	L3	−2.74	0.20	[−3.14 −2.34]	2.80	0.17	[2.47 3.13]	0.06	0.15	[−0.23 0.35]
	L4	−2.42	0.15	[−2.71 −2.12]	2.21	0.06	[2.09 2.33]	−0.21	0.13	[−0.46 0.04]
	L5	−5.79	0.63	[−7.02 −4.55]	2.14	0.23	[1.69 2.60]	−3.64	0.13	[−3.90 −3.39]
D2	L1	−0.26	0.19	[−0.62 0.10]	0.18	0.11	[−0.04 0.39]	−0.08	0.09	[−0.26 0.09]
	L2	−0.83	0.09	[−1.01 −0.65]	0.78	0.28	[0.23 1.33]	−0.05	0.21	[−0.46 0.37]
	L3	−2.50	0.30	[−3.09 −1.91]	2.70	0.33	[2.04 3.35]	0.20	0.15	[−0.09 0.48]
	L4	−1.59	0.27	[−2.13 −1.05]	1.14	0.12	[0.90 1.38]	−0.45	0.33	[−1.09 0.19]
	L5	−1.34	0.20	[−1.74 −0.95]	0.56	0.18	[0.21 0.91]	−0.79	0.19	[−1.15 −0.42]
D3	L1	0.10	0.16	[−0.21 0.41]	0.14	0.13	[−0.11 0.39]	0.24	0.24	[−0.24 0.71]
	L2	1.22	0.30	[0.64 1.81]	0.28	0.26	[−0.23 0.78]	1.50	0.14	[1.23 1.77]
	L3	0.67	0.17	[0.33 1.00]	0.33	0.43	[−0.51 1.18]	1.00	0.37	[0.27 1.73]
	L4	0.36	0.15	[0.07 0.66]	0.13	0.30	[−0.47 0.73]	0.49	0.18	[0.15 0.84]
	L5	0.47	0.08	[0.32 0.63]	0.54	0.23	[0.08 0.99]	1.01	0.17	[0.68 1.34]
D4	L1	−0.12	0.30	[−0.72 0.48]	0.32	0.08	[0.16 0.48]	0.20	0.32	[−0.44 0.83]
	L2	−1.15	0.29	[−1.71 −0.58]	0.03	0.14	[−0.24 0.30]	−1.12	0.18	[−1.48 −0.77]
	L3	−0.48	0.12	[−0.73 −0.24]	−0.08	0.12	[−0.31 0.15]	−0.56	0.06	[−0.67 −0.45]
	L4	0.37	0.10	[0.17 0.57]	0.28	0.22	[−0.15 0.71]	0.65	0.25	[0.16 1.14]
	L5	−1.19	0.12	[−1.42 −0.96]	−0.08	0.12	[−0.30 0.15]	−1.27	0.08	[−1.42 −1.12]
D5	L1	−0.15	0.11	[−0.35 0.06]	0.47	0.11	[0.26 0.68]	0.32	0.06	[0.21 0.43]
	L2	−0.85	0.25	[−1.35 −0.35]	0.83	0.25	[0.34 1.32]	−0.02	0.04	[−0.10 0.07]
	L3	−0.90	0.08	[−1.06 −0.75]	2.08	0.01	[2.06 2.10]	1.18	0.08	[1.03 1.33]
	L4	0.37	0.10	[0.17 0.57]	0.75	0.12	[0.51 0.99]	2.28	0.10	[2.08 2.48]
	L5	−0.44	0.09	[−0.62 −0.26]	0.96	0.13	[0.71 1.21]	0.52	0.07	[0.38 0.66]
D6	L1	−0.99	0.19	[−1.37 −0.61]	0.19	0.15	[−0.11 0.48]	−0.81	0.05	[−0.91 −0.70]
	L2	0.86	0.12	[0.62 1.10]	−0.23	0.18	[−0.59 0.12]	0.63	0.15	[0.33 0.92]
	L3	1.07	0.20	[0.68 1.46]	0.85	0.14	[0.57 1.13]	1.92	0.18	[1.57 2.26]
	L4	−1.62	0.25	[−2.10 −1.14]	0.48	0.18	[0.13 0.83]	−1.14	0.27	[−1.67 −0.61]
	L5	−0.89	0.15	[−1.19 −0.60]	0.95	0.14	[0.67 1.23]	0.05	0.07	[−0.09 0.19]
D7	L1	0.23	0.07	[0.09 0.37]	0.17	0.09	[−0.01 0.36]	0.40	0.09	[0.23 0.58]
	L2	0.56	0.10	[0.36 0.75]	2.21	0.08	[2.05 −1.89]	2.77	0.12	[2.54 2.99]
	L3	−0.08	0.11	[−0.29 0.14]	1.53	0.09	[1.36 1.70]	1.45	0.09	[1.28 1.63]
	L4	−2.68	0.23	[−3.13 −2.22]	2.17	0.12	[1.94 2.40]	−0.51	0.16	[−0.81 −0.20]
	L5	−2.91	0.26	[−3.42 −2.11]	2.60	0.12	[2.36 2.84]	−0.31	0.20	[−0.71 0.09]

Table 4
Mean differences (MD) and lower and upper limits of agreements (95%/± 1.96 Sd) for all distances with overall vertebrae. MD negative values mean the distances measured by the compared method were higher. All values are in mm

	CT-scan Vs MSUS			CAL vs CT-scan			CAL vs MSUS		
	MD	Limits of agreement		MD	Limits of agreement		MD	Limits of agreement	
		Lower	*Upper*		*Lower*	*Upper*		*Lower*	*Upper*
D1	−1.31	*−4.46*	*1.84*	1.40	*−1.32*	*4.13*	0.09	*−0.54*	*0.73*
D2	−1.29	*−3.18*	*0.59*	1.20	*−0.85*	*3.25*	−0.09	*−0.96*	*0.80*
D3	0.59	*−0.58*	*1.70*	0.22	*−0.88*	*1.32*	0.80	*−0.52*	*2.13*
D4	−0.35	*−1.72*	*1.03*	0.14	*−0.50*	*0.77*	−0.21	*−1.80*	*1.38*
D5	−0.09	*−2.16*	*1.97*	1.03	*−0.32*	*2.39*	0.94	*−0.86*	*2.75*
D6	−0.17	*−2.60*	*2.26*	0.32	*−0.67*	*1.31*	0.15	*−2.38*	*2.68*
D7	−0.49	*−3.12*	*2.14*	1.52	*−0.17*	*3.21*	1.03	*−1.46*	*3.52*
Mean	−0.44			0.83			0.39		
SD	0.63			0.55			0.48		

± 0.55 mm and 0.39 ± 0.48 mm for Ct-Scan versus MSUS, CAL versus Ct-Scan and CAL versus MSUS comparison, respectively. These values allow to observe small variations with ultrasound that overestimate distances compared to CT-scan, ultrasound underestimate distances compared to *in situ* measurements and

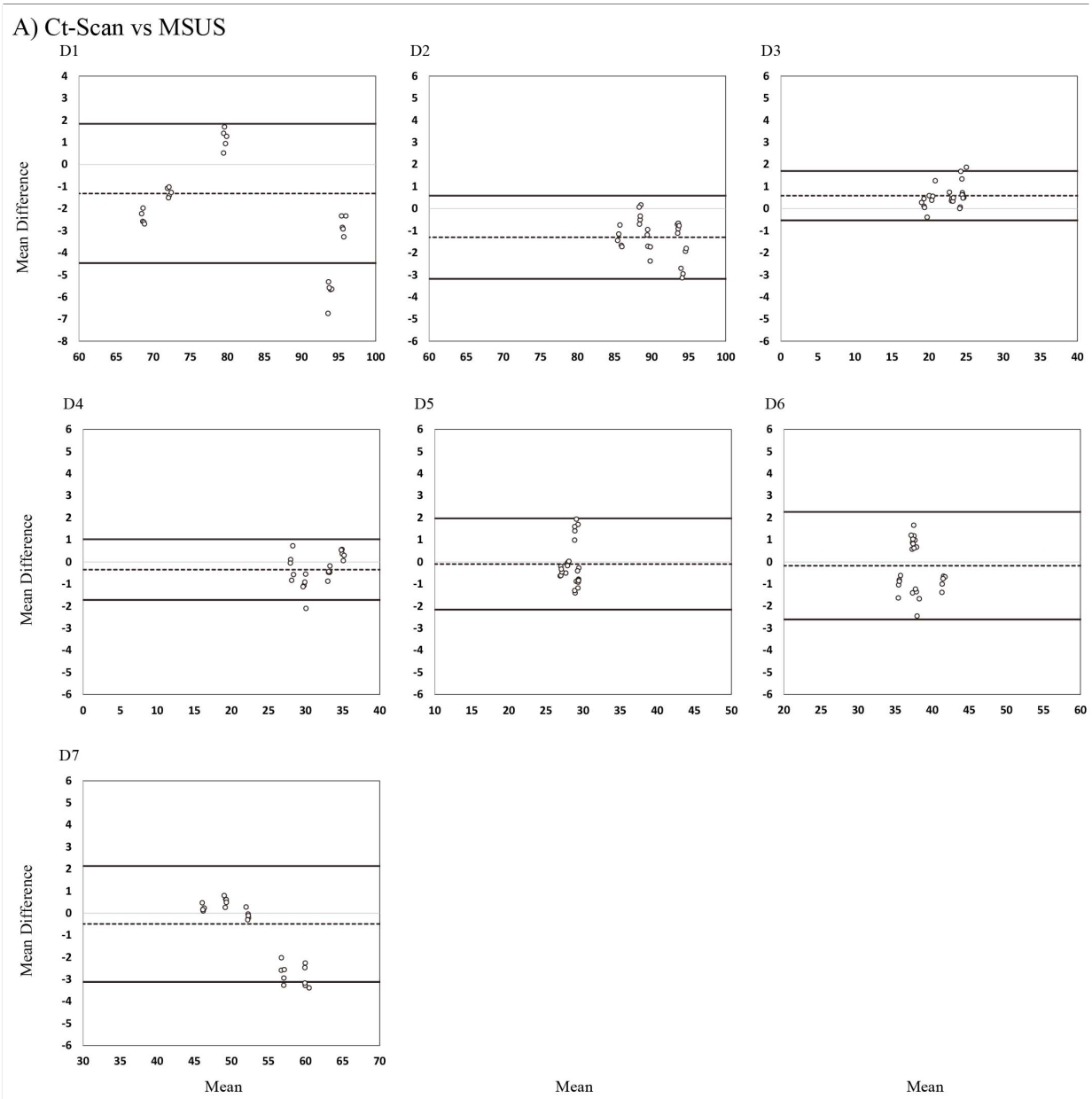

Fig. 5. Bland and Altman plots: A) Ct-Scan and MSUS comparison, B) Ct-Scan and Caliper comparison and C) Caliper and MSUS comparison. Dotted lines refer to the mean differences and continuous lines refer to upper and lower limits of agreement. Values are reported in Table 4.

CT-scan underestimate distances compared to *in situ* measurements.

3.3. MSUS Reliability measurements

Good reliability was observed between each MSUS measurements (Table 5). Mean intra-rater reliability intraclass correlation coefficients for within and between days were 0.970 ± 0.037 and 0.972 ± 0.038, respectively. Concerning the inter-rater reliability, the mean ICC was 0.820 ± 0.212.

4. Discussion

The purpose of this study was to compare the concordance distances measured on 3D modeling of both phantom models (cylinders) and lumbar vertebrae be-

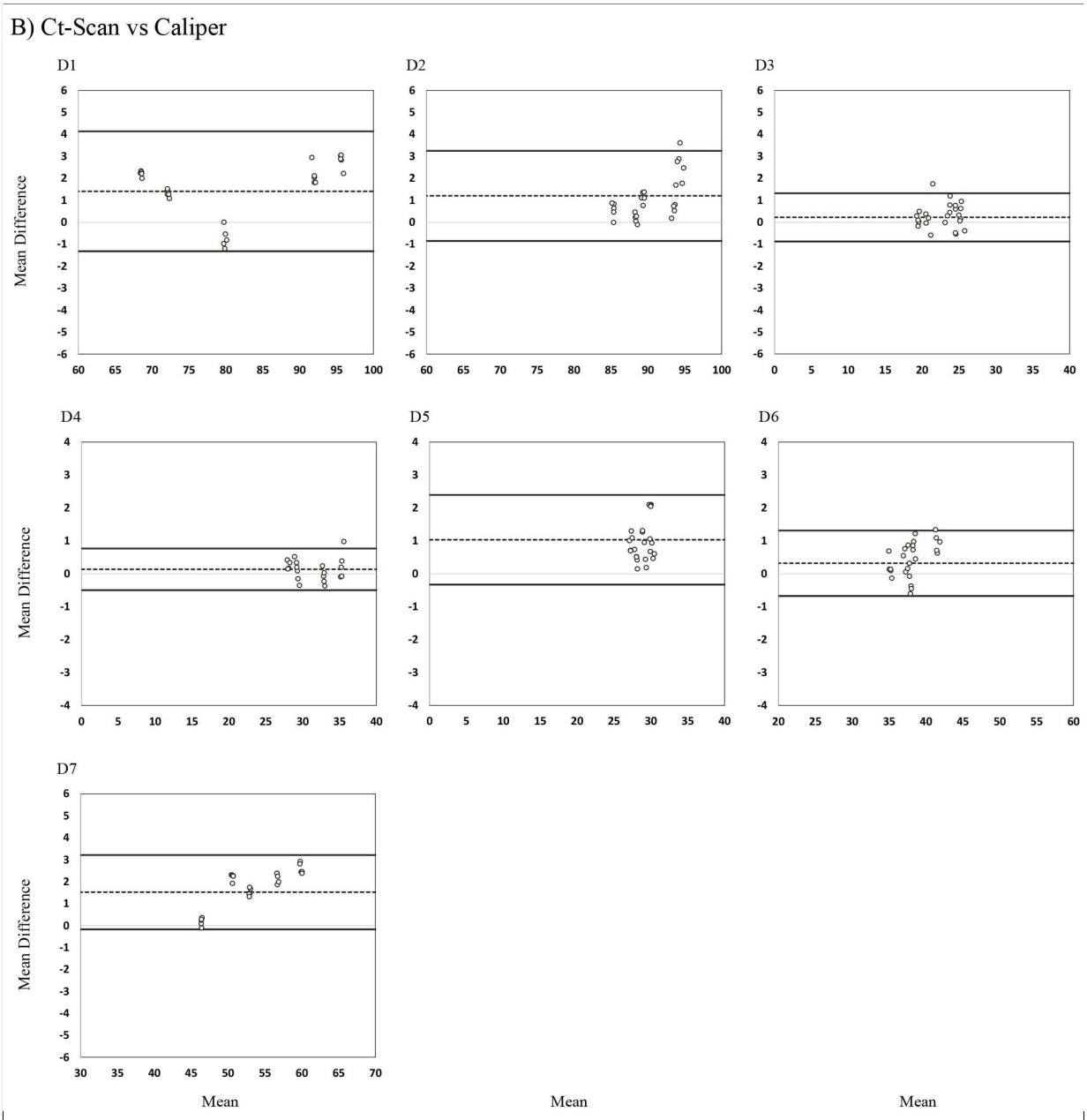

Fig. 5. Continued.

tween CT-scan, MSUS imaging and *in situ* caliper measurements and to study both the intra and inter-reliability distances measurements on 3D bone modeling from MSUS imaging.

Validation on cylinders was the first step. Since characteristics of ultrasound images differ from those obtained by CT-scan, it was necessary at first to acquire images on standardized phantom models in order to develop the method and to define the image reconstruction parameters. In this step, the caliper was considered as gold standard method and we observed on both cylinders, that length and width were almost similar to real distances. Measurements realized on MSUS 3D cylinder modeling seem to be more accurate for cylinders length in comparison to CT-scan. This CT-scan variability could be explained by the increment error during the reconstruction procedure or by the fact the first and the last slice could not be taken at the begin-

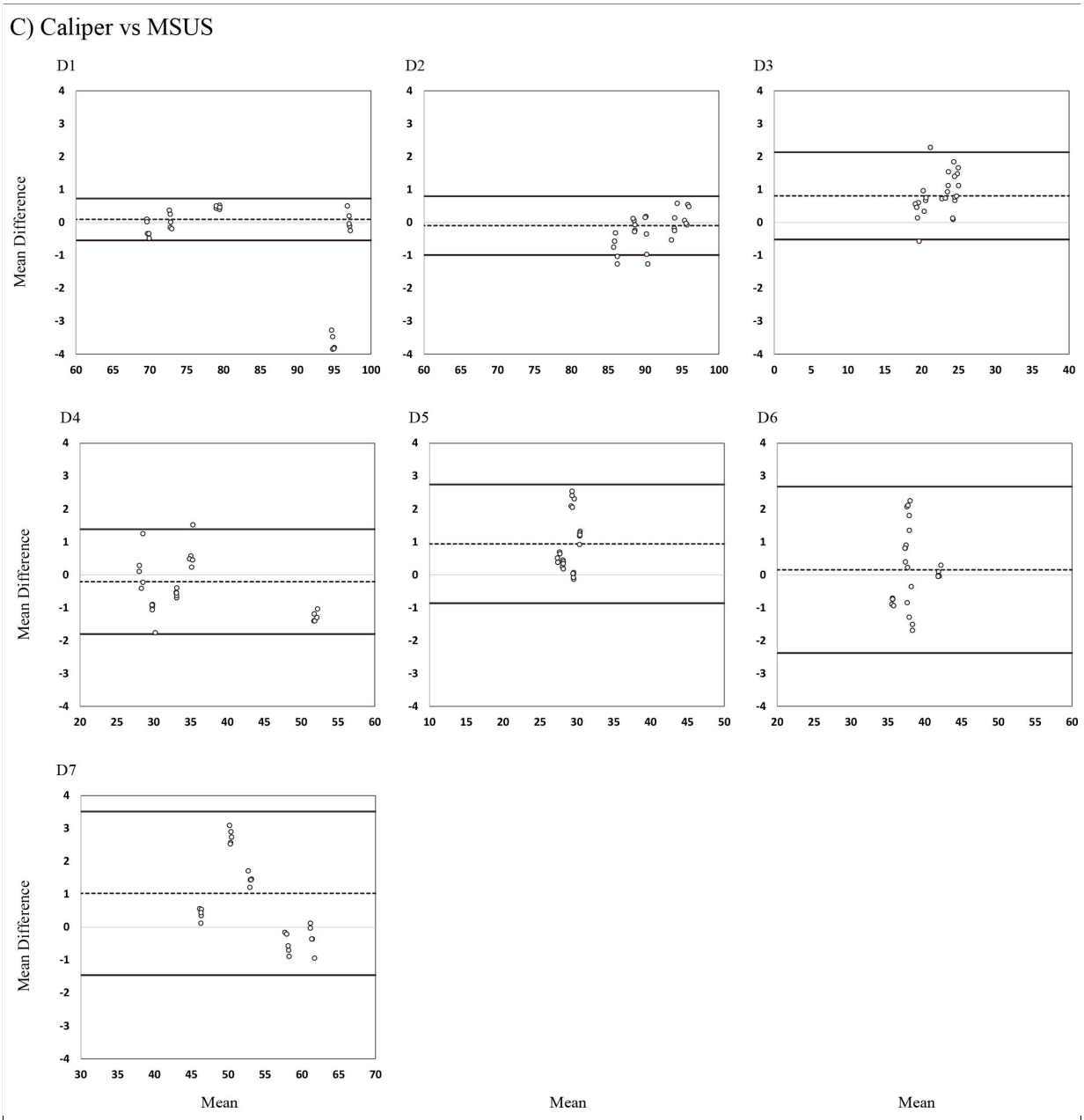

Fig. 5. Continued.

ning and at the end of cylinders during the CT-scan procedure (because of the distance between two slices) giving a higher variation for reconstruction. Concerning width, measurements on CT-scan 3D cylinder modeling were underestimated. This seems to be variable with measurements on 3D cylinder modeling from MSUS but considering the coefficient of variation for both, the length and width, the maximal variations were 0.16% and 0.47%, respectively. These values allowed us to confirm that MSUS method allows to measure with a great precision.

Concerning vertebrae, as the reconstruction method was validated on cylinders, we were able to proceed to the second step which was the application of the same protocol on human lumbar vertebrae. In terms of concordance, results of distances for all vertebrae are within limits of agreement confirming the concordance between CT-scan, MSUS and caliper measurements

Table 5
MSUS intra and inter rater Intraclass correlations coefficient [95% CI]

Distances	Intra rater		Inter-raters
	Within day	Between days	
D1	0.991 [0.981–0.996]	0.993 [0.969–0.999]	0.996 [0.993–0.998]
D2	0.975 [0.951–0.988]	0.981 [0.965–0.991]	0.853 [0.304–0.951]
D3	0.992 [0.954–0.999]	0.991 [0.951–0.999]	0.627 [0.063–0.845]
D4	0.999 [0.998–1.000]	0.999 [0.998–1.000]	0.968 [0.904–0.987]
D5	0.901 [0.532–0.989]	0.900 [0.494–0.989]	0.433 [0.390–0.696]
D6	0.937 [0.710–0.993]	0.940 [0.723–0.993]	0.889 [0.760–0.948]
D7	0.998 [0.992–1.000]	0.998 [0.992–1.000]	0.973 [0.947–0.986]
Mean	0.970	0.972	0.820
SD	0.037	0.038	0.212

(Table 4). Nevertheless, D1 (costiform to costiform) at L5 especially for MSUS measurement were overestimated (Table 3 – MD: -5.79 and -3.64). Even if L5 is the biggest lumbar vertebra it is not the widest. Indeed, L3 is the widest lumbar vertebra (*in situ*: 93 mm for L5 and 97.1 mm for L3 – See D1 Table 2). We know that MSUS overestimate distances and this overestimation could be related to vertebrae width. It seems it is not the case and we have no explanation why the MD for D1 at L5 were higher. Concerning CT-scan, MSUS and CAL, coefficients of variation were ranged from 0.15% to 2.11%, from 0.18% to 3.25% and from 0,05 to 3.42% (Table 2), respectively with Mean CV for CT-scan, MSUS and CAL of 0.67 % $\pm$ 0.49%, 1.11 % $\pm$ 0.93% and 0.58% $\pm$ 0.69%, respectively. These values allow to observe the low variability of measurements for each method. Looking at the mean differences between methods, we observed globally, for all distances that MSUS overestimated distances of $(-)$ 0.44 ± 0.63 mm compared to CT-scan, MSUS underestimated distances of 0.39 ± 0.48 mm compared to *in situ* measurements by caliper and CT-scan underestimated distances of 0.83 ± 0.55 mm compared to *in situ* measurements by caliper (Table 4). These variations were very low regarding lumbar vertebrae size and are acceptable.

Our results seem to be consistent with those of Jia and al. [23] who have presented a computer-aided tracking and motion analysis with ultrasound system to describe hip joint kinematics. They reported a great feasibility of using MSUS in bone segmentation and registration. Although this study differs from ours since it mainly measured hip rotation degrees, the combination of these results suggests that it would be possible to evaluate lumbar kinematics using 3D MSUS modelling.

We also found a good concordance between caliper and ultrasound measurements as previously reported by Sobczak et al. [28], in addition to our findings regarding CT-scan and ultrasound concordance. Finally, our results show a similarity between MSUS, and CT-scan measurement as observed in other studies [33–35] where ultrasound and CT-scan accuracy were compared.

Concerning reliability, a high degree of reliability was observed between each MSUS measurements for intra and inter-rater reliability. Only two measurements for inter-rater reliability showed poorer reliability (D3 and D5). This could be explained by the fact that raters reported greater difficulty in reconstructing and measuring the upper articular surface and the thickness of the vertebral body. Anterior limits of the superior articular process were more difficult to distinguish because of the artifact generated by the fixation rod, and the thickness of the vertebral body was more ambiguous to determine since the bony material was reflected in some images above and below the vertebra. However, vertebral body thickness and superior articular processes are not variables of interest in a context of 3D motion analysis [36] so this measurement error will not be a limit to the pursuit our next studies. We did not assess reliability measurements on 3D bone modeling from CT-scan and *in situ*. We decided to proceed like that because previous study [16] reported that 3D CT-scan modeling was a good method for patient-specific bone modeling for kinematic determination and low-dose computed tomography did not affect 3D bone modeling. In our case, the model of interest was the 3D bone modeling from MSUS and it is why we have determined the reliability of measurements only on this model. Concerning the *in situ* measurements, bone landmarks were well visible and there was any challenge to assess intra and inter reliability on dry vertebrae thanks to the caliper.

Concerning the visual aspect of the 3D reconstructions based on ultrasound images, the results were good and we observed that it is possible to see small structural details. The fact that these reconstructions represent very well the real vertebra is encouraging since it

will be necessary to determine precise bone landmarks to assess both, discrete and later continuous kinematics. Indeed, costiform processes and spinous processes will be of great interest to locate the anatomical coordinate systems. These structures appear very well on MSUS 3D bone modeling and will allow us to accurately locate the vertebral coordinate system.

Determination of joint kinematics dependents of different factors. The first one will be the localizations of bone landmarks on 3D models. An incorrect localization will induce a mispositioning of the anatomical coordinate system inducing alterations of joint displacement with an increase of both, angular (rotation) and linear (translation) displacement [37]. The second factor is the distance between two anatomical coordinate systems. Indeed, the increase of this distance will affect strongly joint translations but will not affect significantly angular displacements. Translation are highly sensitive to the choices of coordinate systems and axes of motion [38].

In the case of a global development of a new method, it was important to compare both ultrasound and CT-scan 3D bone modeling. We first hypothesized that MSUS images would allow a precise 3D modeling of phantom models similar to modelization based on CT-scan, and it would be possible to export the results to vertebrae to open new possibilities in the study of *in vivo* intervertebral motion such as intervertebral both, hypo and hypermobility. Our findings demonstrated a strong concordance in 3D measurements of cylinders and lumbar vertebrae between CT-scan, MSUS imaging and caliper measurements, and a high intra and inter-reliability of 3D MSUS modeling.

The study of *in vivo* joint kinematics is still challenging today. Intracortical pins with external reflective markers are today ethically questionable and impossible to use in clinical practice. Clinical functional assessment using passive or active markers pasted on the skin is acceptable for bigger joints but the artifacts caused by skin movements increase the error of measurement. For small joints, such as intervertebral joint passive markers pasted on the skin will not allow to assess intervertebral displacement. With the improvement of the quality of MSUS images, for example to detect bone fracture [39], MSUS seems to be a good technology to determine, in the future, intervertebral spine displacements.

This study has some limitations. First, only one MSUS acquisition was performed per vertebra. Although the reconstructions were made several times from these images to confirm the reliability, it would have been interesting to have a new acquisition for each 3D reconstruction. Second, in some cases the bone material in the center of the vertebrae (joint facets) was more difficult to distinguish because of the artifact generated by the rod used for stabilization. Third, vertebrae are presented in an ideal environment, as an isolated object in a non-distorting environment (gelatin). Skin, fat, and other tissue could affect the quality of the images, making it difficult to visualize bone limits. The superposition of several images with different angulation should limit this aspect. The next study will have to compare 3D bone modeling from MSUS on the same vertebrae but with and without posterior tissues on several lumbar spine. This will allow to evaluate the effect of the superficial tissues and then assess if tissues induce an alteration of both, bone modeling, then the intervertebral kinematics. The 3D MSU scanning is performed with full access to all sides of the vertebrae. This aspect could be weird because it will be difficult to apply this procedure on patients. First, the intra abdominal fat decrease strongly the quality of MSUS images. Second, to determine spine kinematics, we do not need complete 3D bone models to determine intervertebral displacement. Indeed, as mentioned previously, we need precise localization of bone landmarks and three landmarks are necessary to describe an anatomical coordinate system. In the perspective of spine kinematics, posterior and lateral elements are enough to locate a coordinate system. In this context, readers will find it weird to work on 3D bone modeling from MSUS, since *in vivo*, it will be impossible to access to ventral bone elements but these structures will not be of interest for next studies. The first step was to evaluate if 3D modeling from MSU data set was similar to 3D modeling from tomography. In the future, just the posterior wall of the lumbar spine will be enough to define bone landmarks on partial 3D modeling and define an anatomical coordinate system using spinous processes and lumbar costiform processes.

5. Conclusion

Three-dimensional modeling from 2D ultrasound images of lumbar vertebrae is accurate in comparison to those obtained by CT-scan images and distances measurements were concordant with small errors of measurements. It would therefore be possible to use ultrasound in the study of joint kinematics. Pursuit of research in this direction is necessary to integrate intervertebral motion analysis.

Acknowledgments

The authors thank the Natural Sciences and Engineering Research Council of Canada for the financing of this research project (RGPIN-2016-05717). The authors acknowledge the technicians of the anatomy laboratory, the participants to the body donation program and Camille Dulude for her help with data collection.

Conflict of interest

The authors declare no financial or personal relationships with people or organisations that could have inappropriately influenced this work.

References

[1] U. S. Burden of Disease Collaborators, T. The state of us health, 1990–2016: Burden of diseases, injuries, and risk factors among us states. JAMA, 2018; **319**(14): 1444-1472.

[2] Nunn, M.L., Hayden, J.A., Magee, K. *Current management practices for patients presenting with low back pain to a large emergency department in Canada*. BMC Musculoskelet Disord, 2017; **18**(1): 92.

[3] Panjabi, M.M. *Clinical spinal instability and low back pain*. Journal of Electromyography and Kinesiology, 2003; **13**(4): 371-379.

[4] Cerveri, P., Pedotti, A., Ferrigno, G. *Kinematical models to reduce the effect of skin artifacts on marker-based human motion estimation*. J Biomech, 2005; **38**(11): 2228-36.

[5] Wang, B., et al. *Application of digital orthopedic technology for observing degenerative lumbar segmental instability of three-dimensional kinematic characteristics in vivo*. Zhonghua Yi Xue Za Zhi, 2014; **94**(29): 2264-8.

[6] Pinheiro, A.P., Tanure, M.C., Oliveira, A.S. *Validity and reliability of a computer method to estimate vertebral axial rotation from digital radiographs*. Eur Spine J, 2010; **19**(3): 415-20.

[7] Rezvani, A., et al. *Validity and reliability of the metric measurements in the assessment of lumbar spine motion in patients with ankylosing spondylitis*. Spine (Phila Pa 1976), 2012; **37**(19): E1189-96.

[8] Zuhlke, T., et al. *Accuracy of dynamic computed tomography to calculate rotation occurring at lumbar spinal motion segments*. Spine (Phila Pa 1976), 2009; **34**(6): E215-8.

[9] Emery, D.J., et al. *Management of MRI wait lists in Canada*. Healthcare Policy, 2009; **4**(3): 76-86.

[10] Yeager, M.S., Cook, D.J., Cheng, B.C. *Reliability of computer-assisted lumbar intervertebral measurements using a novel vertebral motion analysis system*. Spine J, 2014; **14**(2): 274-81.

[11] Zhao, K., et al. *Assessment of non-invasive intervertebral motion measurements in the lumbar spine*. J Biomech, 2005; **38**(9): 1943-6.

[12] Zheng, Y., Nixon, M.S., Allen, R. *Automated segmentation of lumbar vertebrae in digital videofluoroscopic images*. IEEE Trans Med Imaging, 2004; **23**(1): 45-52.

[13] Kanagaraj, K., et al. *Assessment of dose and DNA damages in individuals exposed to low dose and low dose rate ionizing radiations during computed tomography imaging*. Mutat Res Genet Toxicol Environ Mutagen, 2015; **789-790**: 1-6.

[14] Sholukha, V., et al. *Double-step registration of in vivo stereophotogrammetry with both in vitro 6-DOFs electrogoniometry and CT medical imaging*. J Biomech, 2006; **39**(11): 2087-95.

[15] Van Sint Jan, S., et al. *Data representation for joint kinematics simulation of the lower limb within an educational context*. Med Eng Phys, 2003; **25**(3): 213-20.

[16] Van Sint Jan, S., et al. *Low-dose computed tomography: a solution for in vivo medical imaging and accurate patient-specific 3D bone modeling*? Clin Biomech (Bristol, Avon), 2006; **21**(9): 992-8.

[17] Della Croce, U., et al. *Human movement analysis using stereophotogrammetry. Part 4: assessment of anatomical landmark misplacement and its effects on joint kinematics*. Gait Posture, 2005; **21**(2): 226-37.

[18] Wang, Q., et al. *Validity study of vertebral rotation measurement using 3-D ultrasound in adolescent idiopathic scoliosis*. Ultrasound Med Biol, 2016; **42**(7): 1473-81.

[19] Hunerbein, M., et al. *Three-dimensional ultrasonography of bone and soft tissue lesions*. Eur J Ultrasound, 2001; **13**(1): 17-23.

[20] Treece, G.M., Gee, A.H., Prager, R.W. *RF and amplitude-based probe pressure correction for 3D ultrasound*. Ultrasound Med Biol, 2005; **31**(4): 493-503.

[21] Kane, D., et al. *Musculoskeletal ultrasound – a state of the art review in rheumatology. Part 1: Current controversies and issues in the development of musculoskeletal ultrasound in rheumatology*. Rheumatology (Oxford), 2004; **43**(7): 823-8.

[22] Delle Sedie, A., Riente, L., Bombardieri, S. *Limits and perspectives of ultrasound in the diagnosis and management of rheumatic diseases*. Mod Rheumatol, 2008; **18**(2): 125-31.

[23] Jia, R., et al. *A computer-aided tracking and motion analysis with ultrasound (CAT & MAUS) system for the description of hip joint kinematics*. Int J Comput Assist Radiol Surg, 2016; **11**(11): 1965-1977.

[24] Abdel Hay, J., Smayra, T., Moussa, R. *Customized polymethylmethacrylate cranioplasty implants using 3-dimensional printed polylactic acid molds: technical note with 2 illustrative cases*. World Neurosurg, 2017; **105**: 971-979 e1.

[25] van den Hoorn, W., et al. *Development and validation of a method to measure lumbosacral motion using ultrasound imaging*. Ultrasound Med Biol, 2016; **42**(5): 1221-9.

[26] Chleboun, G.S., et al. *Measurement of segmental lumbar spine flexion and extension using ultrasound imaging*. J Orthop Sports Phys Ther, 2012; **42**(10): 880-5.

[27] Gercek, E., et al. *Dynamic angular three-dimensional measurement of multisegmental thoracolumbar motion in vivo*. Spine (Phila Pa 1976), 2008; **33**(21): 2326-33.

[28] Sobczak, S., et al. *Reliability and validation of in vitro lumbar spine height measurements using musculoskeletal ultrasound: A preliminary investigation*. J Back Musculoskelet Rehabil, 2016; **29**(1): 171-82.

[29] Zheng, M., et al. *Long-duration tracking of cervical-spine kinematics with ultrasound*. IEEE Trans Ultrason Ferroelectr Freq Control, 2019; **66**(11): 1699-1707.

[30] Bland, J.M., Altman, D.G. *Statistical methods for assessing agreement between two methods of clinical measurement*. Lancet, 1986; **1**(8476): 307-10.

[31] Myles, P.S., Cui, J. *Using the Bland-Altman method to measure agreement with repeated measures*. Br J Anaesth, 2007; **99**(3): 309-11.

[32] Parker, R.A., et al. *Using multiple agreement methods for continuous repeated measures data: a tutorial for practitioners*. BMC Med Res Methodol, 2020; **20**(1): 154.

[33] Huang, X., et al. *Dynamic 2D ultrasound and 3D CT image registration of the beating heart*. IEEE Trans Med Imaging, 2009; **28**(8): 1179-89.

[34] Sprouse, L.R., 2nd, et al. *Is ultrasound more accurate than axial computed tomography for determination of maximal abdominal aortic aneurysm diameter*? Eur J Vasc Endovasc Surg, 2004; **28**(1): 28-35.

[35] Han, S.M., et al. *Ultrasound-determined diameter measurements are more accurate than axial computed tomography after endovascular aortic aneurysm repair*. J Vasc Surg, 2010; **51**(6): 1381-7; discussion 1387-9.

[36] Wu, G., et al. *ISB recommendation on definitions of joint coordinate system of various joints for the reporting of human joint motion – part I: ankle, hip, and spine. International society of biomechanics*. J Biomech, 2002; **35**(4): 543-8.

[37] Morton, N.A., et al. *Effect of variability in anatomical landmark location on knee kinematic description*. J Orthop Res, 2007; **25**(9): 1221-30.

[38] Bull, A.M., et al. *Standardisation of the description of patellofemoral motion and comparison between different techniques*. Knee Surg Sports Traumatol Arthrosc, 2002; **10**(3): 184-93.

[39] O'Brien, A.J., and Moussa, M.A. *Using ultrasound to diagnose long bone fractures*. Journal of the American Academy of PAs, 2020; **33**(2): 33-37.